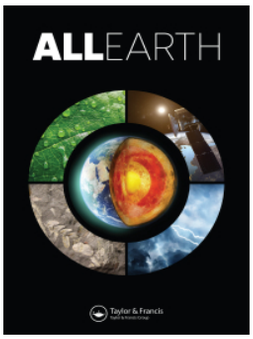

All Earth

ISSN: (Print) (Online) Journal homepage: www.tandfonline.com/journals/tgda21

A statistical collocation accuracy assessment of contemporary satellite temporal gravimetry data products

Wei Chen, Yuhao Xiong, C.K. Shum, Ehsan Forootan, Min Zhong, Jiangjun Ran, Changqing Wang, Wei Feng, Wenhao Li, Zihan Yang & Yingchun Shen

To cite this article: Wei Chen, Yuhao Xiong, C.K. Shum, Ehsan Forootan, Min Zhong, Jiangjun Ran, Changqing Wang, Wei Feng, Wenhao Li, Zihan Yang & Yingchun Shen (2024) A statistical collocation accuracy assessment of contemporary satellite temporal gravimetry data products, All Earth, 36:1, 1-17, DOI: 10.1080/27669645.2024.2399984

To link to this article: https://doi.org/10.1080/27669645.2024.2399984

Published online: 11 Sep 2024.

ALL EARTH
2024, VOL. 36, NO. 1, 2399984
https://doi.org/10.1080/27669645.2024.2399984

Taylor & Francis
Taylor & Francis Group

RESEARCH ARTICLE

OPEN ACCESS Check for updates

A statistical collocation accuracy assessment of contemporary satellite temporal gravimetry data products

Wei Chen[a,b], Yuhao Xiong[c], C.K. Shum[d], Ehsan Forootan[e], Min Zhong[c], Jiangjun Ran[f], Changqing Wang[b], Wei Feng[c], Wenhao Li[g], Zihan Yang[h] and Yingchun Shen[b,c]

[a]College of Resource Environment and Tourism, Hubei University of Arts and Science, Xiangyang, China; [b]State Key Laboratory of Geodesy and Earth's Dynamics, Innovation Academy for Precision Measurement Science and Technology, Chinese Academy of Sciences, Wuhan, China; [c]School of Geospatial Engineering and Science, Sun Yat-sen University, Zhuhai, China; [d]Division of Geodetic Science, School of Earth Sciences, The Ohio State University, Columbus, Ohio, USA; [e]Department of Sustainability and Planning, Aalborg University, Aalborg, Denmark; [f]Department of Earth and Space Science, Southern University of Science and Technology, Shenzhen, China; [g]School of Geomatics Science and Technology, Nanjing Tech University, Nanjing, China; [h]College of Agriculture, Xiangyang Polytechnic, Xiangyang, China

ABSTRACT

The Gravity Recovery and Climate Experiment (GRACE) and GRACE Follow-On (GRACE-FO) missions have enabled consistent production of monthly gravity field solutions by international institutes, contributing to the International Centre for Global Earth Models. Each institute employs distinct processing strategies, yielding varied estimates of terrestrial water storage (TWS). In this study, we employ statistical collocation techniques (Total assessment ratio, TAR) to assess and compare the performance of GRACE TWS data products (2003.03 ~ 2014.03) and GRACE-FO TWS data (2018.06 ~ 2022.11). For GRACE TWS, the TAR values are as follows: COST-G (0.15), ITSG (0.83), APM-SYSU (0.85), CSR (0.91), JPL (0.93), GFZ (0.94), Tongji (0.96), HUST (1.08), SUST (1.18), CNES (1.37), and AIUB (1.41). Similarly, for GRACE-FO TWS, the TAR values are COST-G (0.15), JPL (0.81), ITSG (0.96), CSR (0.97), GFZ (1.06), and CNES (1.41). Furthermore, our comparison across basin sizes and climatic regions reveals that COST-G exhibits lower uncertainty and larger signal-to-noise ratios in TWS, making it particularly noteworthy for its utility. Conversely, other single solutions that depict long-term trends and annual amplitudes demonstrate comparable values across various basin sizes, climatic regions, and specific areas.

ARTICLE HISTORY
Received 22 December 2023
Accepted 29 August 2024

KEYWORDS
Terrestrial water storage (TWS); GRACE/GRACE-FO; total assessment ratio (TAR)

1. Introduction

Terrestrial water storage (TWS), a climate observable distinctly observed by satellite gravimetry data, is a critical component of the global hydrologic cycle and thus provides an invaluable constraint (Huang et al., 2015; Pokhrel et al., 2021; Rodell et al., 2009). Variations in TWS have profound impacts on global surface and groundwater hydrology, and observe the occurrence of extreme hydrological events, e.g. (Daniel et al., 2011, Eicker et al., 2016; Forootan et al., 2019; Kusche et al., 2016). The Gravity Recovery And Climate Experiment (GRACE) mission (2002.04 ~ 2017.06) revolutionised the global TWS monitoring via computing the surface mass load using monthly global gravity field solutions in terms of spherical harmonics coefficients (Tapley et al., 2004). GRACE offered an innovative approach for tracking large-scale changes in TWS, surpassing traditional ground-based observations in both temporal and spatial coverage, leading to numerous hydrological studies using TWS data products (Chen et al., 2022; Scanlon et al., 2016).

Following the decommission of the GRACE mission in October 2017, the GRACE Follow-On (GRACE-FO) twin-satellite mission, launched in May 2018, has been continuing to provide TWS data for diverse geodetic and Earth science applications (Landerer et al., 2020). Notably, the GRACE-FO twin satellites have an experimental laser range interferometry (LRI) satellite-to-satellite instrument, with >50 times more in precision than the operational K/Ka Band microwave ranging (KBR) instrument. Furthermore, advancements in various instrument accuracy and the scientific data system have enhanced the GRACE-FO's ability to detect gravitational variations at a slightly finer resolution, enabling accurate, uniform, and continuous TWS observations, despite the early loss of an accelerometer on one of the GRACE-FO satellites (Landerer et al., 2020).

Monthly gravity field estimates derived from GRACE/GRACE-FO have achieved geoid height undulation precision as fine as 2 to 3 mm at spatial resolutions longer than 286–333 km half-wavelength, corresponding to spherical harmonic coefficients complete to degree 60 and order 60, respectively (Landerer et al.,

CONTACT Yuhao Xiong xiongyh9@mail2.sysu.edu.cn School of Geospatial Engineering and Science, Sun Yat-Sen University, Zhuhai 519082, China

2020; Tapley et al., 2004). The three official GRACE/GRACE-FO Science Data System entities, the Center for Space Research at the University of Texas (CSR), the German Research Center for Geosciences in Potsdam, Germany (GFZ), and the NASA's Jet Propulsion Laboratory (JPL) have been producing monthly global gravity field models. In addition, 8 research institutes have also been contributing publicly available monthly global gravity field models. These institutes include the combined solution from the International Combination Service for Time-variable Gravity Field (COST-G, Jäggi et al., 2020), Graz University of Technology (ITSG, Kvas et al., 2019), Centre national d'études spatiales (CNES, Lemoine et al., 2019), Tongji University (Tongji, Q. Chen et al., 2021), Huazhong University of Science and Technology (HUST, Zhou et al., 2017), Astronomical Institute of the University of Bern (AIUB, Meyer et al., 2016), the Innovation Academy for Precision Measurement Science and Technology of Chinese Academy of Sciences and Sun Yat-sen University (APM-SYSU, Wang et al., 2015), and the Southern University of Science and Technology (SUST, Ran et al., 2014). These centres commonly employ varied processing strategies, resulting in unique noise characteristics in their respective generated spherical harmonic solution (Level 2) derived and mascon solution derived terrestrial water storage (TWS). Here, our goal is to contribute a statistical methodology to evaluate the performance of TWS using various GRACE/GRACE-FO Level 2 data products.

Many prior assessments have focused on comparing subsets of available monthly gravity fields via diverse interdisciplinary applications. For example, Sasgen et al. (2007) focused on Antarctica, highlighting the superior performance of the CNES RL01C product in capturing gravity field changes. Steffen et al. (2009) extended a cautionary note to the use of satellite gravimetry to estimate Fennoscandian glacial isostatic adjustment, emphasising the importance of considering processing methods and selection of hydrological forward model. Chambers and Bonin (2012) contributed to the uncertainty estimates of GRACE-derived ocean bottom observables, by intercomparisons with pressure ocean circulation model outputs. Scanlon et al. (2016) evaluated the performance of GRACE mascon and Level 2 (spherical harmonics) solutions for hydrologic applications, finding similarities but noting the lower performance of CSR and JPL mascon solutions as compared to spherical harmonics. Zhang et al. (2019) delved into the consistency between mascon and spherical harmonics solutions, highlighting mascon solutions' potential for revealing Terrestrial Water Storage (TWS) variations in larger areas but also noting their limitations in smaller regions compared to spherical harmonics. Yao et al. (2019) analysed relative uncertainties in GRACE-derived TWS changes in mainland China and concluded that the CSR Level 2 solution exhibited the lowest uncertainties, particularly for nonseasonal parameters.

However, these evaluations are subject to certain limitations and challenges. The accuracy of models, the extent of coverage provided by hydrological survey stations, and the impact of human activities can introduce uncertainties in the assessments. Additionally, obtaining authentic observations of TWS for evaluating the uncertainty of GRACE/GRACE-FO time-varying gravity field inversion results present a considerable challenge. Therefore, the Three-Cornered Hat (TCH) method which does not necessitate a known real reference field for evaluating the uncertainty of three or more sets of observation sequences (Tavella & Premoli, 1994) and has been successfully applied in diverse contexts, including the evaluation of atmospheric angular momentum products (Koot et al., 2006), fluid load deformation data (Valty et al., 2013), rainfall data (Awange et al., 2016), and also in the assessment of GRACE time-varying gravity field products (Ferreira et al., 2016; Khandu et al., 2016; Long et al., 2017). While the studies employed the TCH method to evaluate GRACE solutions, they may not contain most current publicised and extended time-period GRACE/GRACE-FO products nor conduct a comprehensive analysis from global down to basin-scale assessments. Additionally, the SNR (Signal to Noise Ratio) are also used here to evaluate different products. However, it is difficult to discern which products are better once the uncertainty is lower, and the SNR is greater.

In this study, we introduce a novel statistical assessment ratio known as the 'Total assessment ratio (TAR)', which integrates uncertainty and SNR. Our primary objective is to provide a comprehensive evaluation of the available GRACE/GRACE-FO products across different temporal scales (monthly, seasonal cycle, and the decomposed residuals) and spatial scales (global and basin scale). Additionally, we aim to conduct a comparative analysis of the diverse solutions offered by GRACE/GRACE-FO products in hydrologic applications. The overarching goal of this comprehensive intercomparison of TWS from various institute is potentially provided insights into the robustness of each data product's processing and post-processing strategies.

2. Data and methods

2.1. Global major river basins

A total of 89 river basins have been meticulously selected to represent a range of aridity and humidity intensities, as depicted in Figure 1. The basin areas, totalling 7.36×10^7 km^2, were sourced from the Global Aridity Index and Potential Evapotranspiration (ET0) Climate Database v2 (accessed on 15 June 2023,

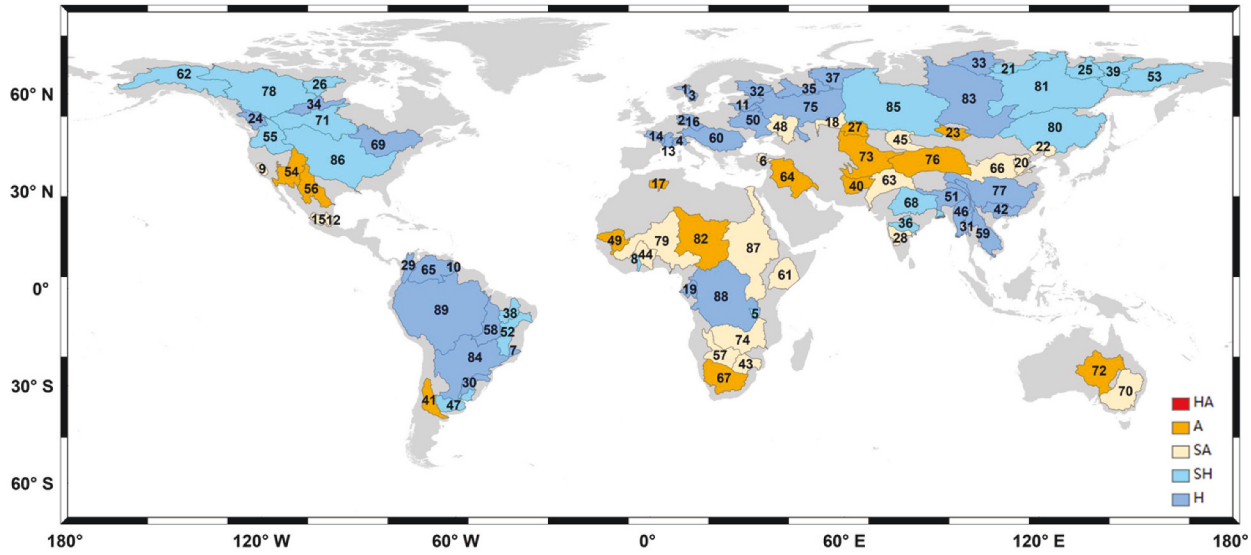

Figure 1. Locations and humidity of study basins. Humidity is characterised by Aridity Index (AI).

https://figshare.com/articles/dataset/Global Aridity Index and Potential Evapotranspiration ET0 Climate_Database_v2/7504448/3). These river basins were categorised into size classes, comprising large (40 basins, >500,000 km^2), medium (36 basins, 100,000–500,000 km^2) and small (13 basins 40,000–100,000 km^2). The global humidity was further classified into five categories (Trabucco & Zomer, 2019), namely Arid (A: $0.03 < AI < 0.2$, 14 basins), Semi-arid (SA: $0.2 < AI < 0.5$, 20 basins), Sub-humid (SH: $0.5 < AI < 0.65$, 20 basins), and Humid (H: $AI > 0.65$, 35 basins).

2.2. GRACE/GRACE-FO level-2 products

In our comprehensive assessments, the newly publicised Level-2 (gravity solutions expressed in spherical harmonics) datasets are included (Table 1) by 11 research institutes, namely, CSR, GFZ, JPL, COST-G, ITSG, CNES, Tongji, HUST, AIUB, APM-SYSU, and SUST. The majority of these datasets are available from the International Centre for Global Earth Models (ICGEM), (http://icgem.gfz-potsdam.de/home, accessed 15 March 2023). The GRACE data obtained from the three official institutions (CSR, JPL, and GFZ) are of the RL06 version, whereas the GRACE-FO data corresponds to the RL06.1 version. Conversely, for COST-G, the GRACE data pertains to the RL01 version, while the GRACE-FO data aligns with the RL02 version. For other institutions, these version numbers for products were not specified. Although the various data products span at different time periods, we used the 11 research institutes (CSR, GFZ, JPL, COST-G, ITSG, CNES, Tongji, HUST, AIUB, APM-SYSU, and SUST) for GRACE solutions covering a common data span, 2003.04–2014.03, for the comparison study. For the evaluation of GRACE-FO data products, we compared the solutions produced by six institutes (CSR, GFZ, JPL, COST-G, ITSG, and CNES) from June 2018 to November 2022.

Table 1. GRACE/GRACE-FO product information from 11 institutions.

Institutions	Versions	Time span
CSR	GRACE RL06	2002.04-2016.08
	GRACE-FO RL06.1	2018.06-2022.11
GFZ	GRACE RL06	2002.04-2016.08
	GRACE-FO RL06.1	2018.06-2022.11
JPL	GRACE RL06	2002.04-2016.08
	GRACE-FO RL06.1	2018.06-2022.11
COST-G	GRACE RL01	2002.04-2016.08
	GRACE-FO RL02	2018.06-2022.11
ITSG	GRACE 2018	2002.04-2016.08
	GRACE-FO OP	2018.06-2022.11
CNES	GRACE RL05	2002.04-2016.08
	GRACE-FO RL05	2018.06-2022.11
Tongji	GRACE 2022	2002.04-2016.12
HUST	GRACE 2020	2003.01-2016.07
AIUB	RL02	2003.03-2014.03
APM-SYSU	/	2003.01-2015.12
SUST	/	2003.04-2010.12

('/' indicates that there is currently no version number available.).

The post-processing of both GRACE and GRACE-FO data involved a meticulous sequence of steps: (1) Replacement of the degree-1 (Sun et al., 2016), C20 (Cheng et al., 2011), and C30 coefficients (Loomis et al., 2020). (2) Adopting the GGM05C gravity field model as the reference model (http://download.csr.utexas.edu/pub/grace/GGM05/). (3) Correction of the Glacial Isostatic Adjustment (GIA) geophysical processed using the ICE-6G_D (VM5a) model (Peltier et al., 2015). (4) Mitigation of north-south stripe errors through the application of decorrelation filters (DDK3) (Kusche et al., 2009). (5) Computation of the surface mass change expressed in density of water via Farrell's loading (Wahr et al., 1998), and then (6) resample the gridded TWS with 0.5°×0.5° via simple interpolations.

2.3. Three-Cornered hat method

Three-Cornered Hat (TCH) method shares similarities with the triple collocation approach (Stoffelen, 1998). However, it is important to note that the triple collocation method is designed for calculating uncertainties involving three variables, whereas the TCH method is versatile and can handle more than three variables. The TCH method has been demonstrated to be invaluable for estimating the relative uncertainties associated with TWS derived from different products within the GRACE missions.

The time series of TWS at each grid point for a specific time epoch are represented as $\{X_i\}_{i=1,2,\ldots,N}$. In this scenario, N is equal to the number of products, comprising three products from the GRACE/GRACE-FO Science Data System (SDS) processing centres, namely CSR, GFZ and JPL, and eight additional solutions from COST-G, ITSG, CNES, Tongji, HUST, AIUB, APM-SYSU and SUST, respectively. X_i is the sum of true value (X_t) and the error (ε_i),

$$X_i = X_t + \varepsilon_i \quad i = 1, \ldots, N \tag{1}$$

To calculate the error (ε_i), TCH algorithm is employed here. The differences among N-1 products can be defined as:

$$Y_{i,M} = X_i - X_{reference} = \varepsilon_i - \varepsilon_N, \quad i = 1, \ldots, N-1 \tag{2}$$

$X_{reference}$ is the reference time series, which is arbitrarily chosen from the time series X_i. Y is an M×(N-1) matrix, N represents the number of products being compared, and M signifies the length of the time series. The covariance matrix of Y can be expressed as:

$$S = \mathrm{cov}(Y) \tag{3}$$

The unknown N×N covariance matrix of the individual noise R is related to S as:

$$S = J \cdot R \cdot J^T \tag{4}$$

where J is the $(N-1) \times N$ identity matrix with an additional column of −1s appended, can be expressed by

$$J_{N-1,N} = \begin{bmatrix} 1 & 0 & \cdots & 0 & -1 \\ 0 & 1 & \cdots & 0 & -1 \\ \vdots & \vdots & \vdots & \vdots & \vdots \\ 0 & 0 & 0 & \cdots & -1 \end{bmatrix} \tag{5}$$

For the equation (2), it cannot be solved as the number of unknown elements is greater than the number of equations. To address this, we introduce the Kuhn – Tucker theorem proposed by Galindo and Palacio (1999) to constrain the minimisation problem. The objective function can be defined as:

$$F(r_{1N} \ldots r_{NN}) = \frac{1}{K^2} \sum_{i<j}^{N} r_{ij}^2 \tag{6}$$

and the corresponding constraint function is:

$$H_{(r_{1N} \ldots r_{NN})} = -\frac{R}{|S| \cdot K} < 0 \tag{7}$$

where $r_{1N} \ldots r_{NN}$ are the elements of Q, and $K = \sqrt[N-1]{|S|}$. The initial conditions for the iteration are:

$$r_{iN}^0 = 0, i < N; r_{NN}^0 = \frac{1}{2 \cdot S^*}; \tag{8}$$

$$S^* = [1, \ldots, 1] \cdot S^{-1} \cdot (1, \ldots, 1)^T \tag{9}$$

Finally, the matrix Q can be obtained by minimising the objective function in the equation (4). The square root of the diagonal values Q is the uncertainty of evaluated TWS. The solved uncertainty to the mean of TWS is the relative uncertainty.

2.4. Performance metrics

Calculating the signal-to-noise ratio (SNR) aids in understanding the intensity of the results of each GRACE/GRACE-FO product relative to the background noise. SNR can be obtained by the following equation:

$$SNR = 10 \times \log_{10}\left(\frac{P_{signal}}{P_{noise}}\right) \tag{10}$$

$$P_{signal} = \frac{1}{N} \sum_{i=1}^{N} TWS_i^2 \tag{11}$$

P_{signal} is the root mean square (RMS) of each grid value of TWS. P_{noise} represents the uncertainty estimated by the TCH method.

It is challenging to determine which product is superior when the uncertainty is lower, but the SNR is greater. To address this, we introduce the total assessment ratio (TAR) as the final performance metric, calculated as follows:

$$Total = \sqrt{(uncertainty_{Rescale})^2 + (WSNR_{Rescale})^2} \tag{12}$$

Here, $uncertainty_{Rescale}$ denotes that the value of uncertainty is rescaled to the range of 0.1 ~ 1; $WSNR_{Rescale}$ is the value of $WSNR$ which is also rescaled to the range of 0 ~ 1; $WSNR$ can be computed using the following formula:

$$WSNR = \frac{sum(SNR) - SNR}{sum(SNR)} \tag{13}$$

A smaller value of TAR indicates better performance for the product.

2.5. Time series decomposition

TWS can be decomposed into trends, seasonal cycles, and interannual variations, as follows:

$$TWS = TWS_{trend} + TWS_{annual} + TWS_{semi-annual} + Residuals \quad (14)$$

The mathematical formulation of time series decomposition method is:

$$TWS = a \cdot t + b1 \cdot \cos(\omega_1 \cdot (t+\psi_1)) + b2(2\omega_2 \cdot (t+\psi_2)) + \varepsilon \quad (15)$$

where **a** represents the trend of TWS; b1 and b2 denote the annual amplitude and semi-annual amplitude, respectively; ψ_1 and ψ_2 represent the annual phase and semi-annual phase, respectively; ε is the residual or interannual variations of TWS.

3. Results

3.1. Assessments of GRACE estimated TWS

Three performance metrics, including uncertainty, SNR, and TAR, are utilised to analyse the performance of TWS from 11 GRACE products: CSR, GFZ, JPL, COST-G, ITSG, CNES, Tongji, HUST, AIUB, APM-SYSU, and SUST. Figure 2 illustrates the uncertainty of GRACE TWS globally. COST-G exhibits the lowest uncertainty on a global scale, while CNES, AIUB, and SUST obviously display greater uncertainty. In specific regions, CSR, HUST, JPL, GFZ, and SUST show higher uncertainty in eastern Antarctica; Tongji, HUST, JPL, APM-SYSU, and GFZ display higher uncertainty in the Amazon; Tongji also presents higher uncertainty in the middle-latitude area; JPL and APM-SYSU show greater uncertainty in Tibetan Plateau regions and parts of Africa; CSR exhibits higher uncertainty on the western Australia coast and southeastern Canada. A comprehensive summary of uncertainty for various products is provided in Table 2. COST-G boasts the lowest uncertainty at 0.35 cm, while AIUB (1.99 cm), CNES (1.87 cm), and SUST (1.56 cm) have higher uncertainty. Other institutions fall in the middle range, ranging from 0.96 cm to 1.20 cm.

Figure 3 presents the SNR globally, highlighting COST-G's higher signal intensity in most terrestrial areas, contrasting with lower values for AIUB and CNES, particularly in western Russia, the centre of Africa, and South Asia. The higher SNR patterns are associated with regions experiencing significant water loss or gain and seasonal fluctuations. A detailed summary of SNR values is provided in Table 2, with COST-G achieving the highest value at 17.44, while CNES (11.28) and AIUB (11.31) record the lowest values. APM-SYSU (13.37), ITSG (13.25), CSR (13.08), JPL (13.07), Tongji (12.78), HUST (12.20), and SUST (11.93) exhibit comparatively strong signal.

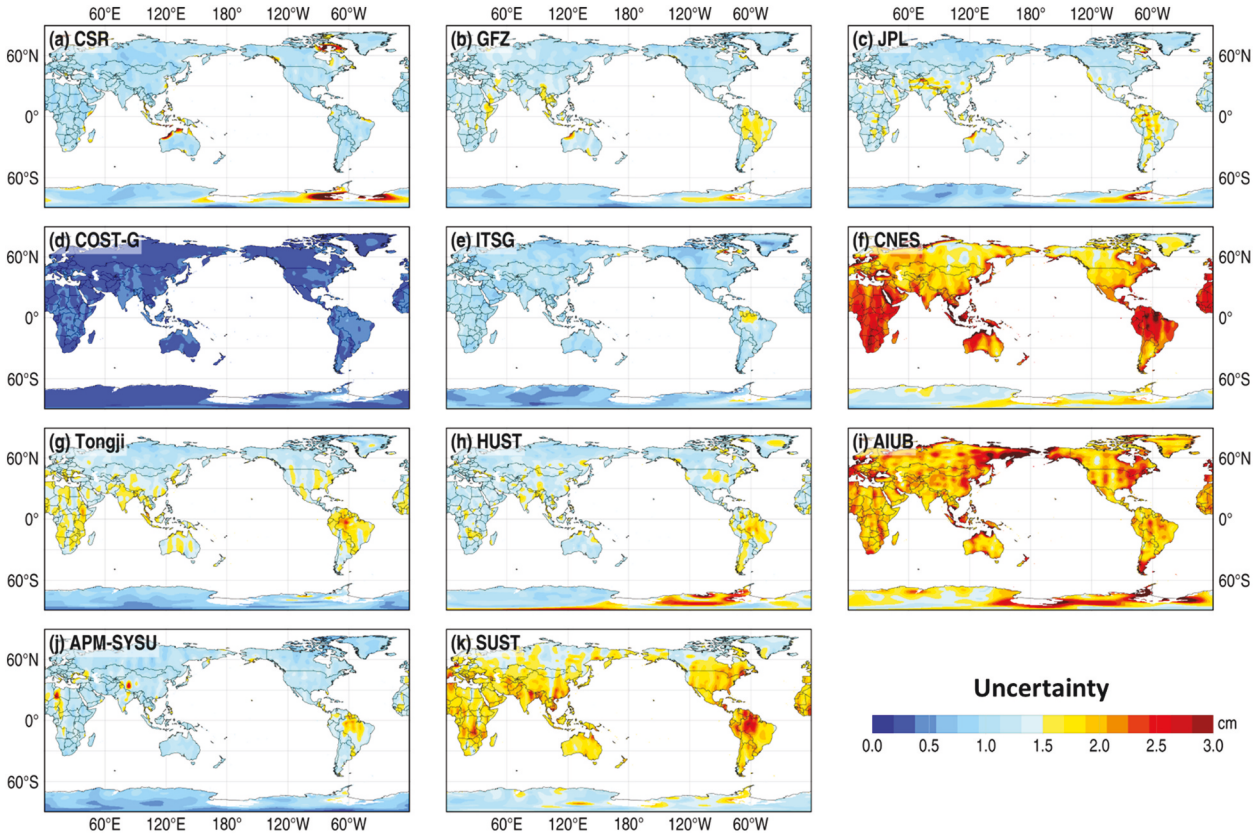

Figure 2. For GRACE product, the uncertainty of global TWS obtained by TCH method are presented in (a) CSR, (b) GFZ, (c) JPL, (d) COST-G, (e) ITSG, (f) CNES, (g) Tongji, (h) HUST, (i) AIUB, (j) APM-SYSU, and (k) SUST, respectively.

Table 2. For GRACE TWS in the same time span, the uncertainty, SNR, and TAR of various institutions.

Institutions	Uncertainty(cm)	SNR	TAR
CSR	1.13	13.08	0.91
GFZ	1.16	12.84	0.94
JPL	1.16	13.07	0.92
COST-G	0.35	17.44	0.15
ITSG	0.96	13.25	0.83
CNES	1.87	11.28	1.37
Tongji	1.20	12.78	0.96
HUST	1.35	12.20	1.08
AIUB	1.99	11.31	1.41
APM-SYSU	1.07	13.37	0.85
SUST	1.56	11.93	1.18

Considering cases where uncertainty is higher, but SNR is greater, it's difficult to discern the better product. To address this, the TAR, introduced as a comprehensive ratio, aids in the evaluation (see Figure 4). TAR values reflect the overall performance, with lower values indicating better performance in GRACE TWS. COST-G stands out with the lowest TAR, indicating superior performance, while CNES, AIUB, and SUST present higher TAR values than other products. Notably, APM-SYSU, CSR, JPL, and ITSG exhibit better performance in Greenland, and APM-SYSU outperforms other institutions significantly in Antarctica. Table 2 provides a summary of TAR, with COST-G leading with the best TAR at 0.15, followed by ITSG (0.83), APM-SYSU (0.85), CSR (0.91), JPL (0.92), GFZ (0.94), Tongji (0.96), HUST (1.08), SUST (1.18), CNES (1.37), and AIUB (1.41).

3.2. Assessments of GRACE-FO estimated TWS

Among the GRACE-FO level-2 products, assessments are limited to six institutions: CSR, GFZ, JPL, COST-G, ITSG, and CNES. Figure 5 shows the uncertainty of GRACE-FO TWS globally. Notably, COST-G exhibits the lowest uncertainty, while CNES displays greater uncertainty. In specific regions, GFZ and ITSG present greater uncertainty than CSR and JPL in middle latitude area; GFZ shows higher uncertainty than CSR, GFZ and ITSG in Greenland; CSR, JPL, and GFZ exhibit higher uncertainty than ITSG in Antarctica. A comprehensive summary of uncertainty for various products is provided in Table 3. COST-G boasts the lowest uncertainty at 0.45 cm, while CNES (2.17 cm) has the highest uncertainty. Other institutions fall in the middle range between 1.14 cm and 1.51 cm. Figure 6 presents the SNR of GRACE-FO TWS globally. COST-G exhibits higher SNR than other institutions. The signal mainly concentrates in regions exhibiting greater water loss or gain, such as Greenland, Antarctica, western Canada, and India, and areas with significant seasonal variations, such as the Amazon and the centre of Africa. A summary of SNR values for various products is provided in Table 3.

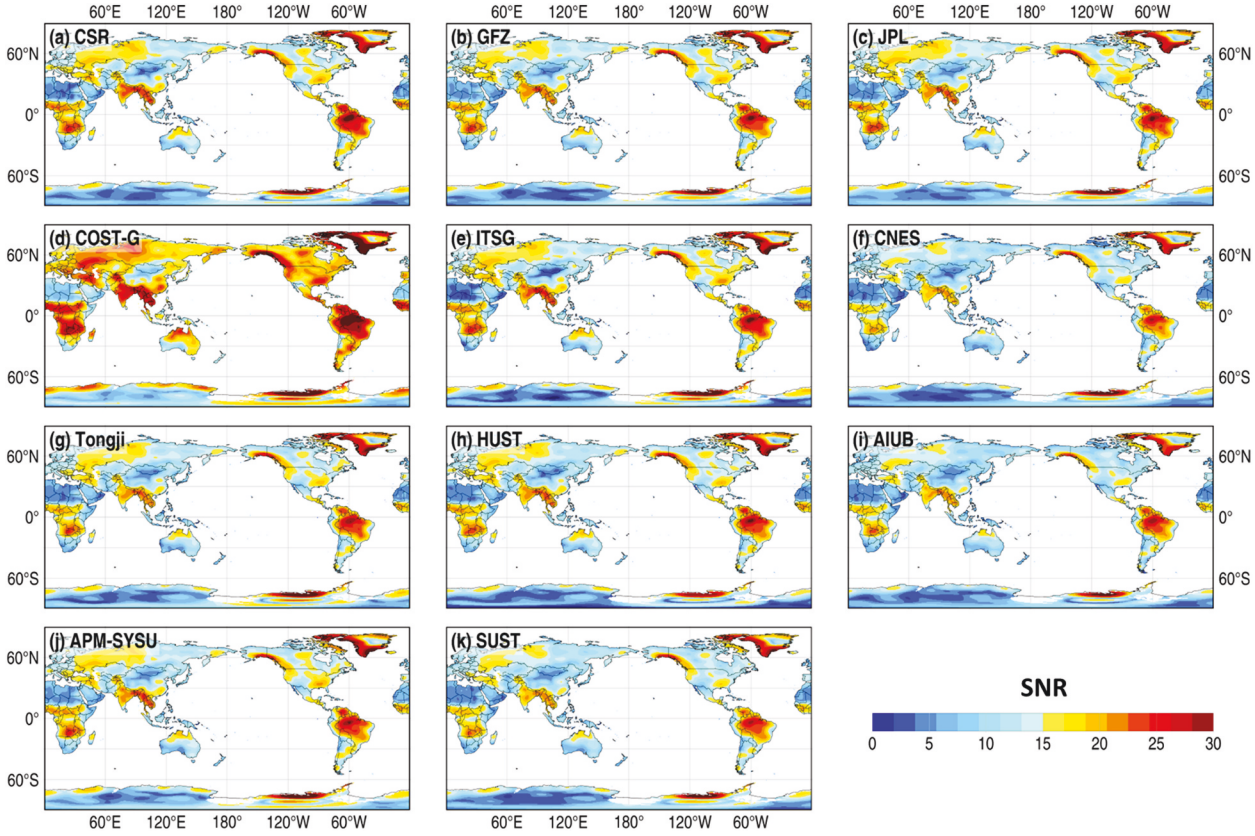

Figure 3. For GRACE product, the SNR of global TWS are presented in (a) CSR, (b) GFZ, (c) JPL, (d) COST-G, (e) ITSG, (f) CNES, (g) Tongji, (h) HUST, (i) AIUB, (j) APM-SYSU, and (k) SUST, respectively.

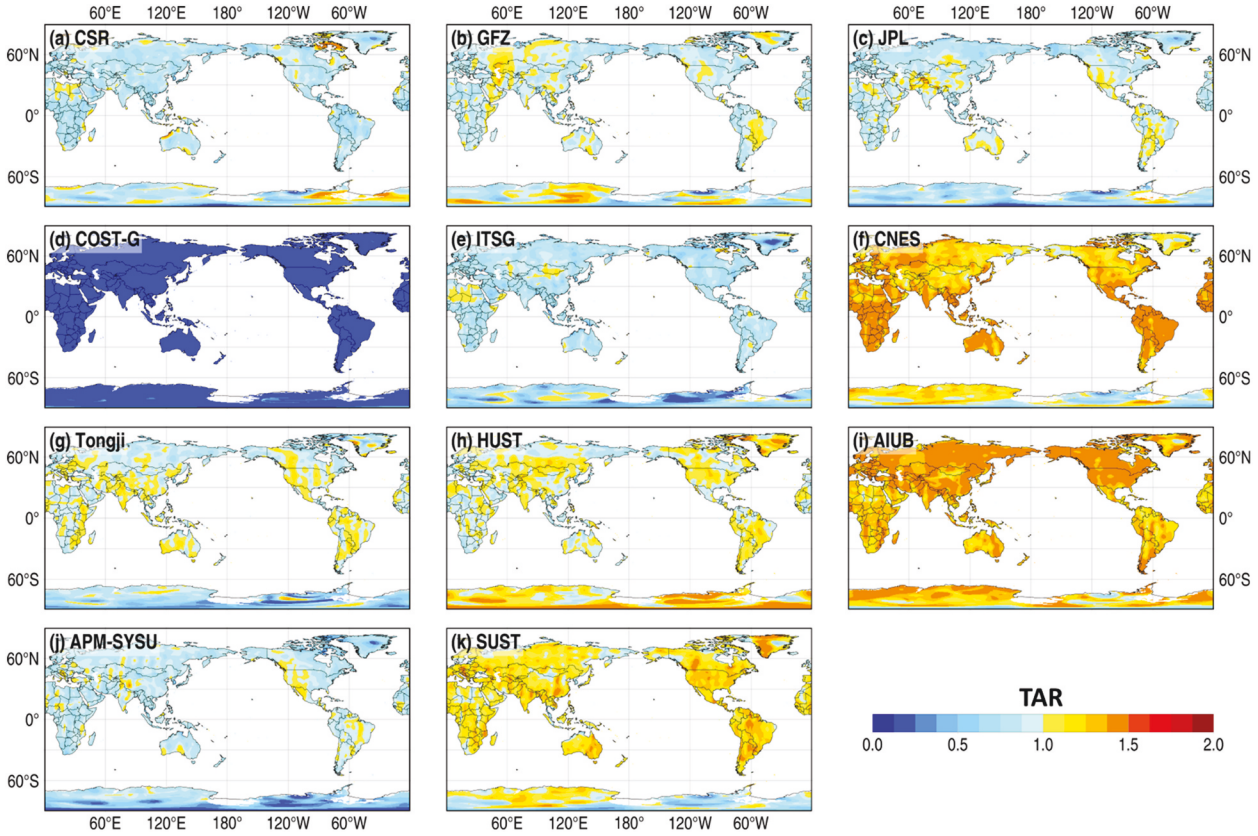

Figure 4. For GRACE product, the TAR of global TWS is presented in (a) CSR, (b) GFZ, (c) JPL, (d) COST-G, (e) ITSG, (f) CNES, (g) Tongji, (h) HUST, (i) AIUB, (j) APM-SYSU, and (k) SUST, respectively.

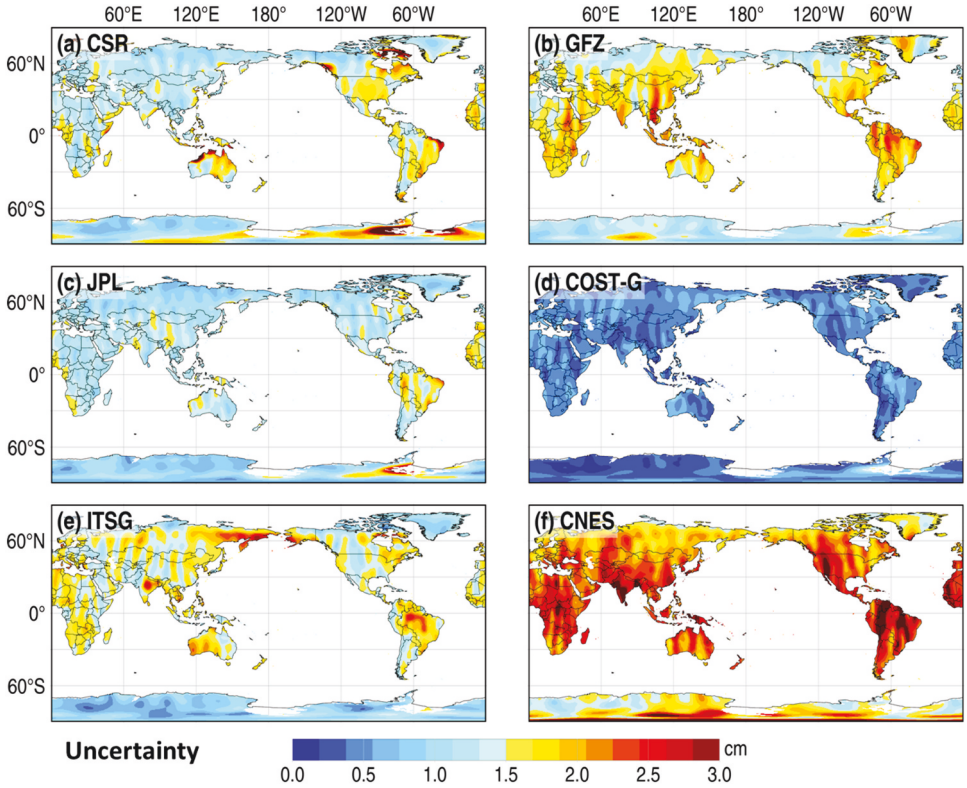

Figure 5. For GRACE-FO product, the uncertainty of global TWS obtained by TCH method are presented in (a) CSR, (b) GFZ, (c) JPL, (d) COST-G, (e) ITSG, and (f) CNES, respectively.

Table 3. For GRACE-FO TWS in the same time span, the uncertainty, SNR, and TAR of various institutions.

Institutions	Uncertainty(cm)	SNR	TAR
CSR	1.37	19.01	0.97
GFZ	1.51	18.62	1.06
JPL	1.14	19.76	0.81
COST-G	0.45	23.67	0.15
ITSG	1.35	18.99	0.96
CNES	2.17	17.43	1.41

COST-G attains the highest value at 23.67, followed by JPL (19.376), CSR (19.01), ITSG (18.99), GFZ (18.62), and CNES (17.43).

Figure 7 denotes the value of TAR: COST-G stands out with the lowest TAR, signifying superior performance, while CNES presents higher TAR values than other products. In Antarctica, ITSG and JPL exhibit better performance than CSR and GFZ. In Greenland, JPL and ITSG present better performance than GFZ and CSR. Table 3 provides a conclusive summary of the performance metrics, where COST-G stands out with the best performance (TAR: 0.15), followed by JPL (0.81), ITSG (0.96), CSR (0.97), GFZ (1.07), and CNES (1.41).

In terms of the value of uncertainty, the results in GRACE-FO TWS are greater than GRACE TWS. However, the intensity of the signal in GRACE-FO TWS is higher than GRACE TWS. Above all, the TAR of GRACE-FO TWS is higher than GRACE TWS, which is probably attributable to the absence of an accelerator in the GRACE-FO satellites. For GRACE and GRACE-FO derived TWS, JPL presents better performance than other institutions, followed by COST-G.

3.3. Comparisons in the decomposed GRACE/GRACE-FO TWS

The time series of TWS are usually decomposed into trends, seasonal terms, and residuals (or interannual variations). First, we present the trend and annual amplitude of GRACE/GRACE-FO TWS from the aforementioned six institutions in Figures 8 and 9, respectively. They collectively reveal water increase or loss in targeted regions, such as glacier ablation in Greenland, the Antarctic Peninsula, West Antarctica, and the Gulf of Alaska coast; groundwater depletion in the Northwest India Aquifer and the North China Plain; freshwater accumulation in far-northern North America and Eurasia, as well as in the wet tropics; reservoirs filling in the Three Gorges regions; precipitation increase in parts of Africa, the Amazon, Australia, and southern China. Additionally, these institutions capture higher annual amplitude, predominantly in the Amazon, India, Mainland Southeast Asia, the centre of Africa, and the Gulf of Alaska coast. The trend of global TWS is presented in Table 4, showing minimal differences among these solutions. For the annual amplitude, the results from six institutions also remain consistent. This suggests that all these solutions effectively capture the global rate and annual amplitude of TWS.

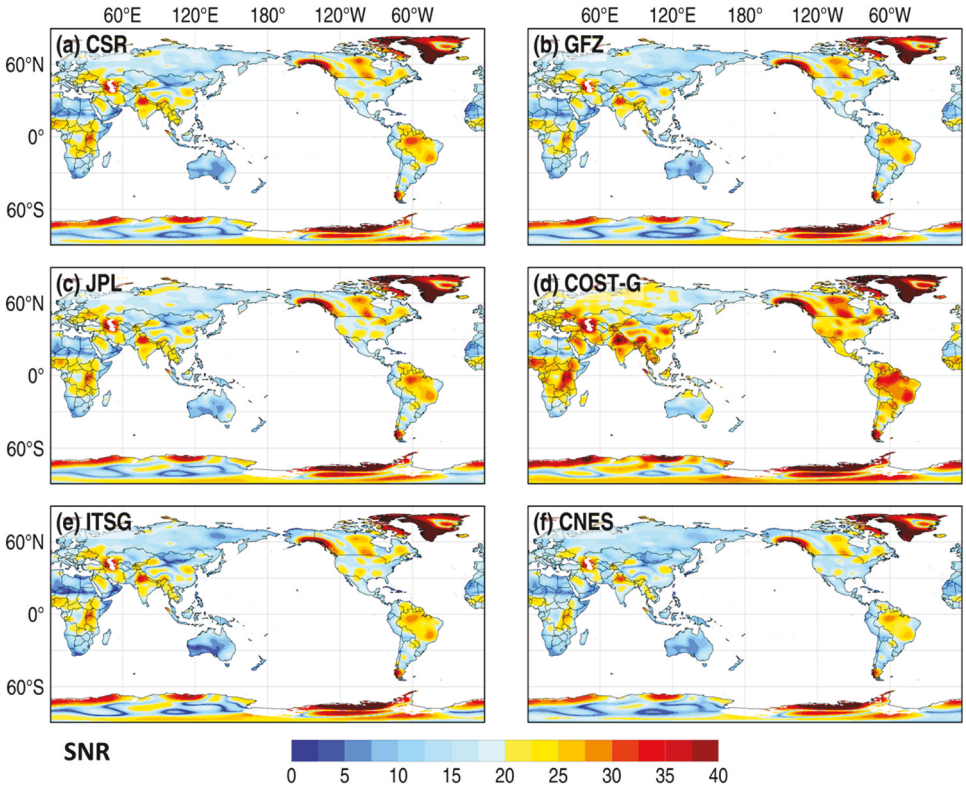

Figure 6. For GRACE-FO product, the SNR of global TWS is presented in (a) CSR, (b) GFZ, (c) JPL, (d) COST-G, (e) ITSG, and (f) CNES, respectively.

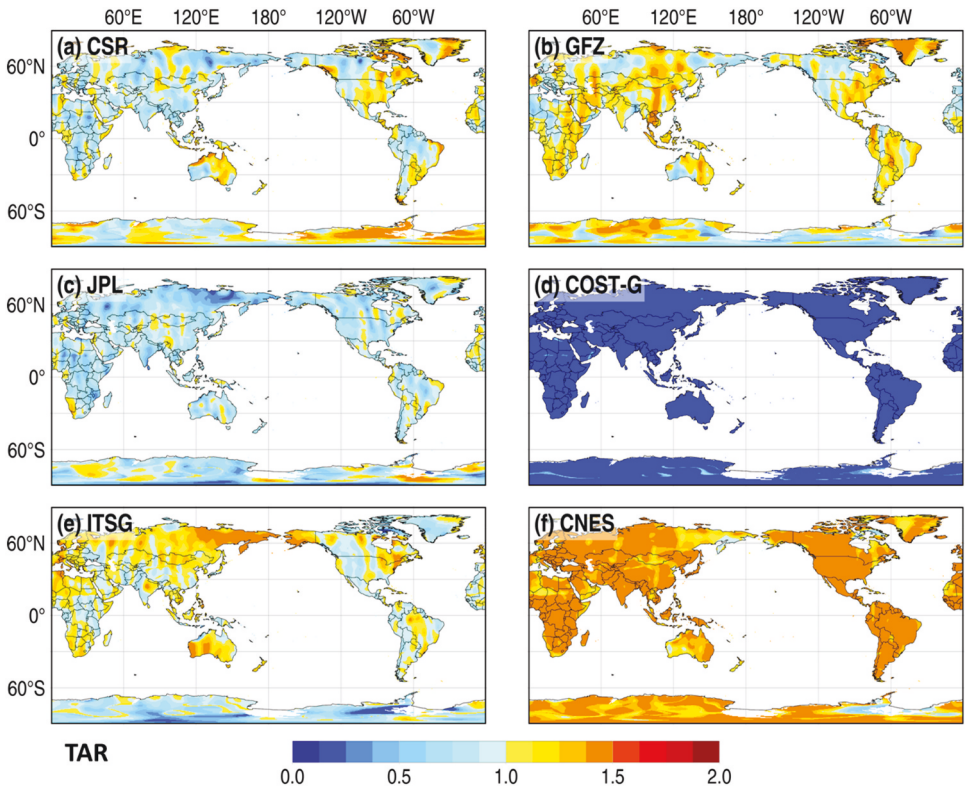

Figure 7. For GRACE-FO product, the TAR of global TWS is presented in (a) CSR, (b) GFZ, (c) JPL, (d) COST-G, (e) ITSG, and (f) CNES, respectively.

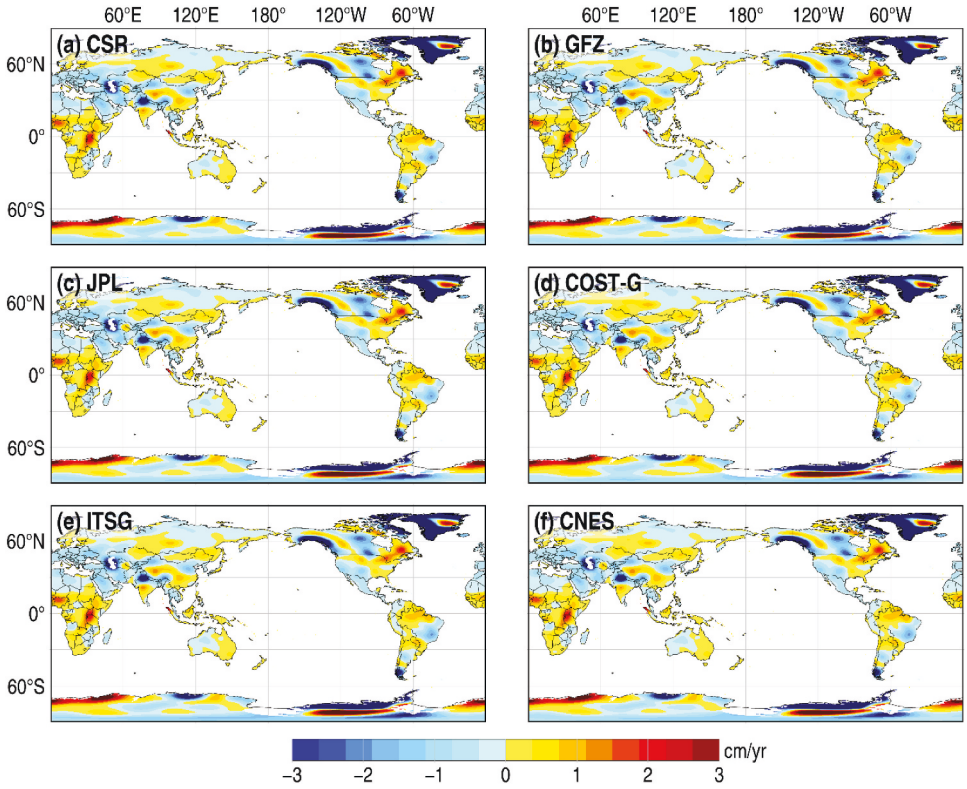

Figure 8. For GRACE/GRACE-FO product, the trend of global TWS is presented in (a) CSR, (b) GFZ, (c) JPL, (d) COST-G, (e) ITSG, and (f) CNES, respectively.

Then, we assess the decomposed cycle and residual components extracted from the global TWS time series (see Tables 5 and 6). Specifically, for the seasonal term, our focus is on the annual and semi-annual signals, each exhibiting uncertainties well below the submillimeter range, significantly surpassing the accuracies of

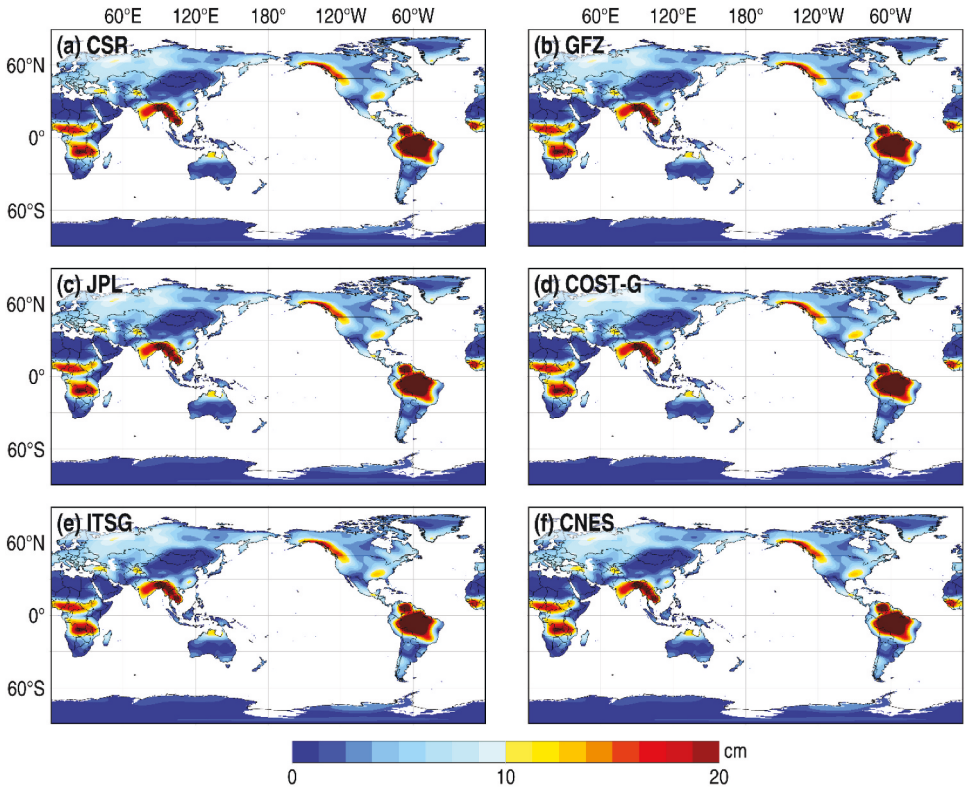

Figure 9. For GRACE/GRACE-FO product, the annual amplitude of global TWS is presented in (a) CSR, (b) GFZ, (c) JPL, (d) COST-G, (e) ITSG, and (f) CNES, respectively.

Table 4. The trend and annual amplitude of GRACE/GRACE-FO TWS.

Institutions	Trend (cm/yr)	Annual amplitude (cm)
CSR	−0.32	2.14
GFZ	−0.31	2.17
JPL	−0.32	2.15
COST-G	−0.33	2.13
ITSG	−0.33	2.17
CNES	−0.33	2.16

Table 5. For the seasonal term of GRACE/GRACE-FO TWS, the uncertainty, SNR, and TAR of various institutions.

Institutions	Uncertainty(cm)	SNR	TAR
CSR	0.01	22.22	0.18
GFZ	0.06	15.93	1.41
JPL	0.02	20.79	0.44
COST-G	0.02	19.70	0.56
ITSG	0.01	22.31	0.17
CNES	0.01	22.59	0.14

Table 6. For the interannual variations of GRACE/GRACE-FO TWS, the uncertainty, SNR, and TAR of various institutions.

Institutions	Uncertainty(cm)	SNR	TAR
CSR	0.08	4.73	0.77
GFZ	0.16	1.82	1.32
JPL	0.05	6.40	0.52
COST-G	0.03	9.80	0.14
ITSG	0.09	4.62	0.81
CNES	0.18	1.63	1.41

GRACE/GRACE-FO TWS. Regarding SNR, it registers a lower value compared to other institutions, whereas CNES outperforms its counterparts. In terms of TAR, CNES (0.14) and ITSG (0.17) demonstrate lower values than other institutions, with GFZ (1.41) recording a higher value. For the interannual variations, the uncertainty is higher than the seasonal cycle, and the signal intensity is lower. In terms of the summary assessments of TAR, COST-G stands out with the best performance (TAR: 0.14), followed by JPL (0.52), CSR (0.77), ITSG (0.81), GFZ (1.32), and CNES (1.41). By comparing the assessment ratio between the original time-series and correspondingly decomposed components, it suggests that the evaluation ratio of original TWS is mainly influenced by the interannual variations.

3.4. The comparisons in catchment scale

Furthermore, we evaluate GRACE/GRACE-FO TWS derived from various solutions in global major basins. Figure 10 shows the boxplot detailing the uncertainty, SNR, and TAR across 89 basins. COST-G emerges as the top performer, showcasing an average ratio of uncertainty (0.22 cm), SNR (24.16), and TAR (0.14). Conversely, CNES, with an uncertainty of 1.84 cm, SNR of 15.12, and TAR of 1.41, fails to demonstrate superior conditions compared to other institutions. CSR (TAR: 0.88), JPL (TAR: 0.89), and ITSG (TAR: 0.92) exhibit almost identical performance across 89 basins, all outperforming GFZ (TAR: 1.07). The assessments of GRACE/GRACE-FO TWS are also conducted in small, medium, and larger basins (see Figure 11). Regardless of the basin size, COST-G consistently outperforms other institutions; there are little differences among

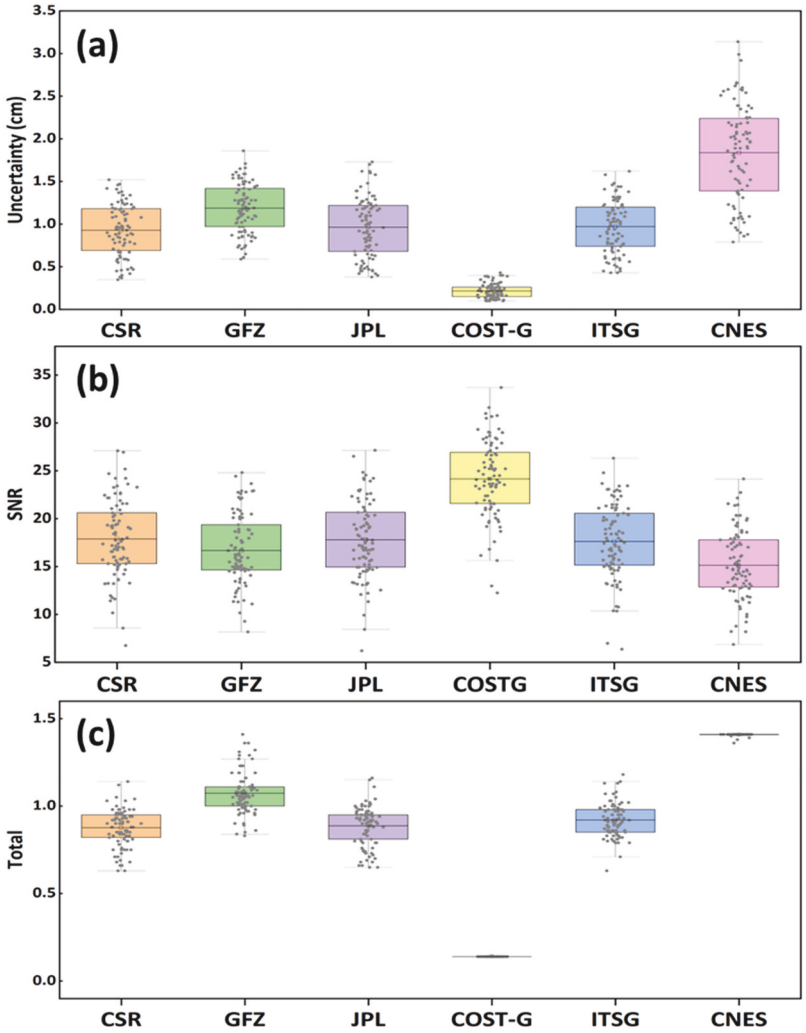

Figure 10. In 89 divided basins, boxplot of uncertainty (a), SNR (b), and TAR (c) in GRACE/GRACE-FO TWS among six products.

CSR, JPL, and ITSG, then followed by JPL and CNES. For uncertainty, medium basins exhibit higher values, whereas small basins show lower values, possibly due to fewer changes in TWS in smaller basins. In terms of SNR, larger basins display greater signal intensity. However, the summary ratio of TAR remains stable, irrespective of basin size.

Meanwhile, we present the uncertainty, SNR, and TAR of GRACE/GRACE-FO TWS in different climatic area, Arid, Semi-Arid, Semi-Humid, and Humid basins (see Figure 12). COST-G consistently demonstrates superior performance, there are also little differences among CSR, JPL, and ITSG, then followed by JPL and CNES. All above, the uncertainty is comparatively lower in Humid basins; the signal is slightly stronger in Semi-humid basins.

4. Temporal gravimetry data products in hydrologic applications

Determining actual uncertainties and SNR for GRACE and GRACE-FO data remains challenging due to the absence of independent estimates of TWS, the TAR and TCH method offer an alternative approach for the evaluation of TWS derived from different solutions. Remarkably, COST-G consistently demonstrates superior performance on a global scale, across basins of various sizes, and in diverse climatic regions when compared to alternative solutions. This superiority is attributed to COST-G's integration of the majority of publicly available GRACE/GRACE-FO data provided by ICGEM, enabling the generation of monthly gravity fields with reduced systematic errors. The amalgamation of the considered time series in COST-G results are in lower noise levels compared to other solutions.

While other solutions may not match COST-G in terms of assessment ratios, it should be noted that this doesn't imply their solutions lack utility in studying hydrologic applications: long-term trends, seasonal changes, and interannual variations. Figure 13 depicts the trend and annual amplitude in small, medium, and large basins, respectively. These solutions all capture a water increase at a rate of ~0.11 cm/yr in small basins, while medium and large basins experience water loss at rates of −0.29 cm/yr and −0.34 cm/yr, respectively. Annual amplitude exhibits minimal variation among institutions, with GFZ displaying slightly lower values. Figure 14 showcases the trend and annual amplitude

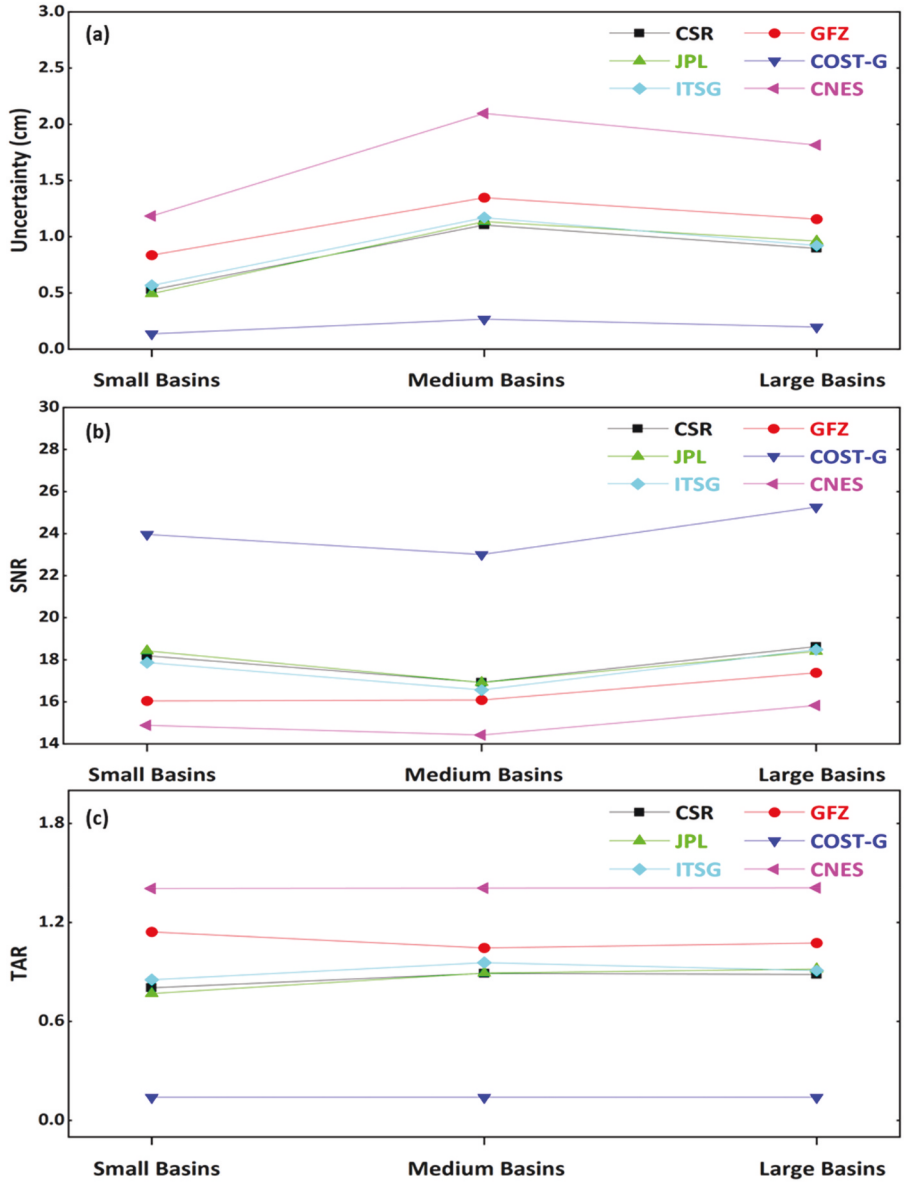

Figure 11. The uncertainty (a), SNR (b), and TAR (c) of GRACE/GRACE-FO TWS in small, medium, and large basins, respectively.

in various climatic areas. All solutions exhibit similar water decrease in these climatic basins. The rate is lower in semi-arid basins, greater in semi-humid and humid areas. The annual amplitude of arid basins is higher than other climatic basins, with semi-arid and semi-humid basins exhibiting roughly similar values. The results show that demonstrate the comparable performance in CNES to capture the rates of water change and annual amplitude, although its assessment ratios are not as favourable as others. Also, the results in sections 3.3 and 3.4 reveal that these solutions exhibit globally consistent spatial patterns, along with numerically similar long-term trends and annual amplitudes, irrespective of area size or climatic region. Additionally, consistency in seasonal signals among different solutions is higher for the magnitude of seasonal amplitudes than for long-term trends.

Furthermore, three distinct areas – the Amazon Basin (dominated by the seasonal cycle), North China Plain (dominated by long-term trends) and Murray Basin (dominated by interannual variations) are assessed here (see Figure 15). In the Amazon Basin, minimal differences (below the submillimeter) in annual amplitude are observed. In the North China Plain, rates of long-term groundwater depletion range from −1.13 to −1.27 cm/yr. In the Murray Basin, the fluctuations in TWS are evidently linked to El Niño Southern Oscillation (ENSO) events (Wu et al., 2022, 2023).

Indeed, despite the variations in error or uncertainty levels among the different GRACE/GRACE-FO Level-2 products, we should recognise that these solutions hold value for hydrologic applications whether applied on a global scale or at the basin level. Their utility extends to understanding long-term trends, seasonal changes, and the dynamics of water storage in different climatic and geographical regions. The evaluation methods and assessment

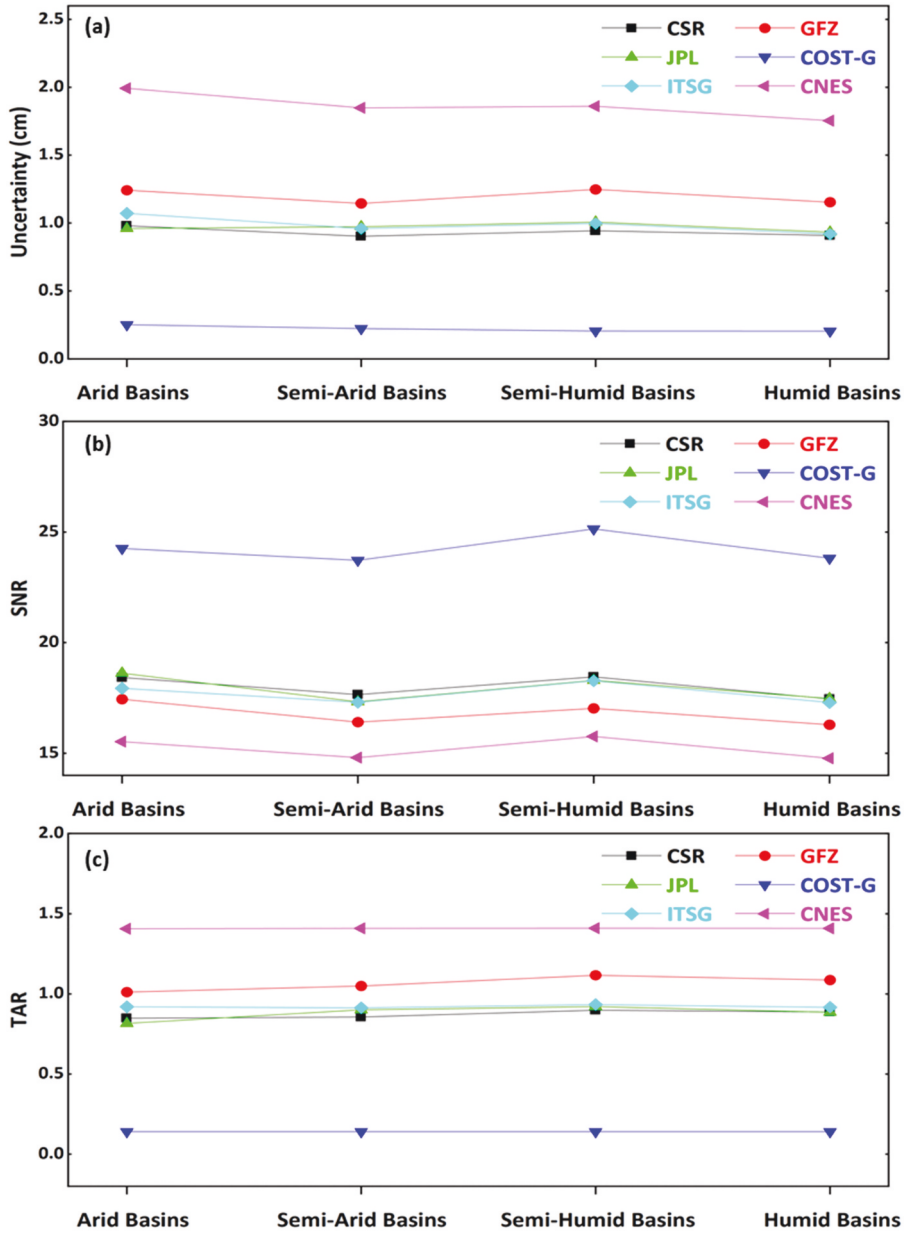

Figure 12. The uncertainty (a), SNR (b), and TAR (c) of GRACE/GRACE-FO TWS in arid, semi-arid, semi-humid, and humid basins, respectively.

ratios offer a means to compare and interpret the performance of various solutions. In light of the assessments conducted, we recommend the preferential use of COST-G products.

5. Conclusions

In this study, we undertook a comprehensive assessment of TWS derived from released GRACE and GRACE-FO Level-2 products, evaluating various performance metrics, including uncertainty, SNR, and the TAR ratio. The assessment encompassed CSR, GFZ, JPL, COST-G, ITSG, CNES, Tongji, HUST, AIUB, APM-SYSU, and SUST.

For GRACE-derived TWS, COST-G exhibited the lowest uncertainty at 0.35 cm, while AIUB (1.99 cm), CNES (1.87 cm), and SUST (1.56 cm) demonstrated higher uncertainty. SNR values ranged from COST-G with the highest at 17.44 to CNES (11.28) and AIUB (11.31) with the lowest. APM-SYSU, ITSG, CSR, JPL, Tongji, HUST, and SUST exhibited comparatively strong signals. The TAR ratio ranked COST-G the best at 0.15, followed by ITSG (0.83), APM-SYSU (0.85), CSR (0.91), JPL (0.92), GFZ (0.94), Tongji (0.96), HUST (10.8), SUST (1.18), CNES (1.37), and AIUB (1.41). For GRACE-FO derived TWS, COST-G again showcased the lowest uncertainty at 0.45 cm, while CNES (2.17 cm) had the highest uncertainty. SNR values ranged from COST-G with the highest at 23.67 to CNES (17.43). COST-G maintained its superior performance in TAR (0.15), followed by JPL (0.81), ITSG (0.96), CSR (0.97), GFZ (1.06), and CNES (1.41). The TAR of GRACE-FO TWS was higher than GRACE TWS. JPL outperformed other institutions for both GRACE and GRACE-FO derived TWS, followed by COST-G.

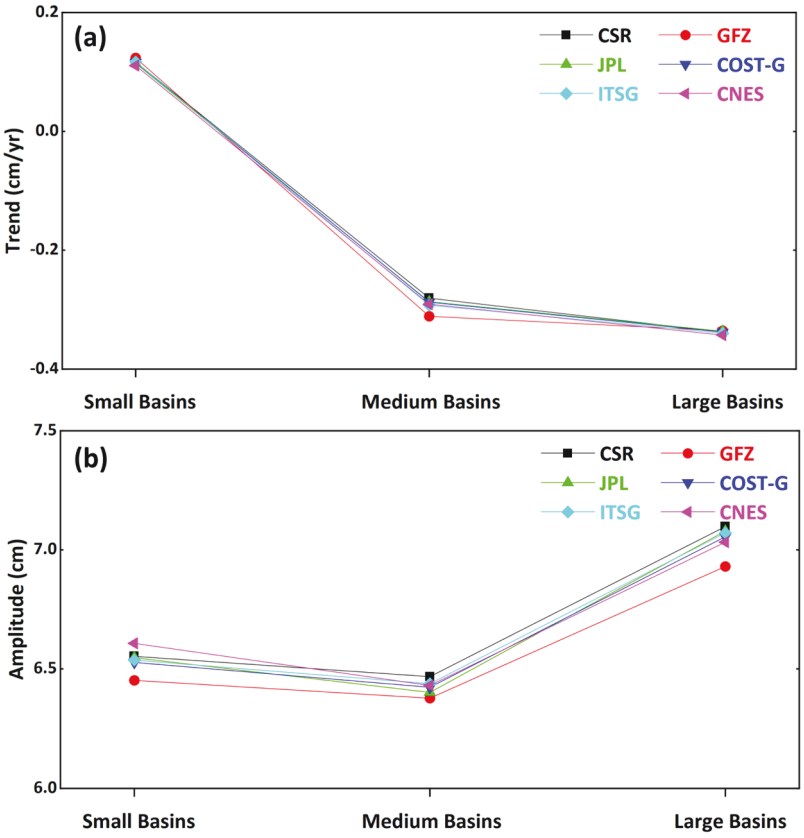

Figure 13. Trend (a) and amplitude (b) of GRACE/GRACE-FO TWS in small, medium, and large basins, respectively.

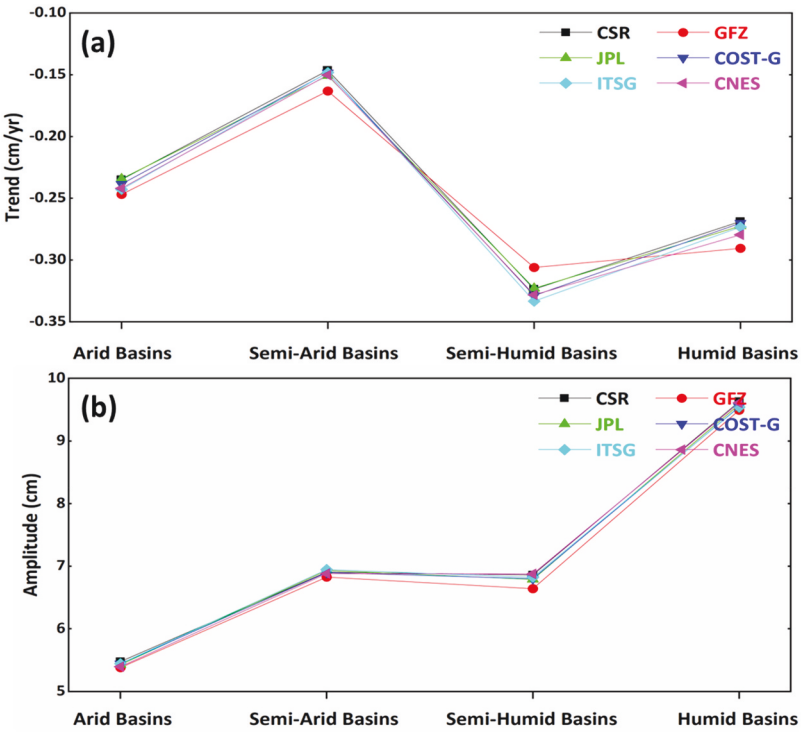

Figure 14. Trend (a) and amplitude (b) of GRACE/GRACE-FO TWS in arid, semi-arid, semi-humid, and humid basins, respectively.

Furthermore, the assessment extended to trends, cycles, and residuals of GRACE/GRACE-FO TWS. For the seasonal term, uncertainties were well below the sub-millimeter range. SNR values showed variations, with GFZ recording a lower value compared to other institutions, and CNES outperforming its counterparts. In terms of TAR, CNES (0.14) and ITSG (0.17) demonstrated lower values, while GFZ (1.41) recorded a higher value. The evaluation ratio of original TWS was primarily dominated by interannual variations. We also assessed

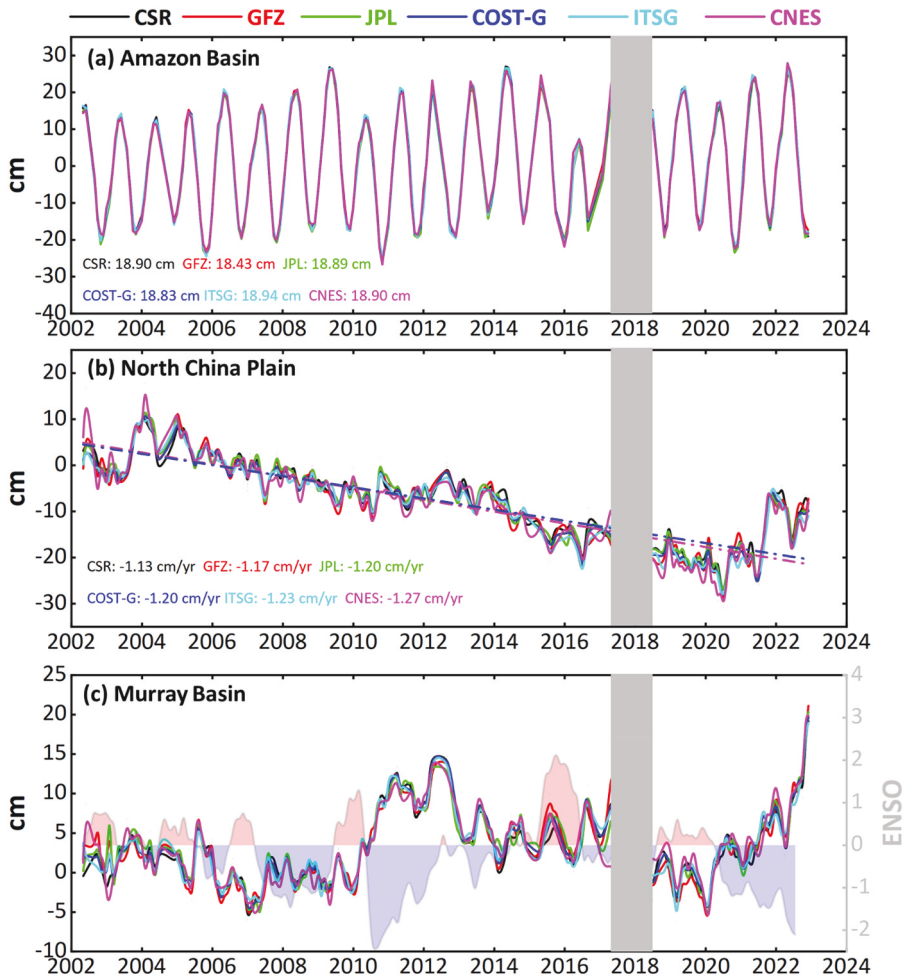

Figure 15. The results of six solutions in Amazon Basin (a), North China plain (b), and Murray Basin (c), respectively.

GRACE/GRACE-FO TWS in 89 major basins which revealed COST-G as the top performer, displaying an average ratio of uncertainty (0.22 cm), SNR (24.16), and TAR (0.14). Conversely, CNES did not demonstrate superior conditions compared to other institutions. The assessments whether in different size basins or various climatic areas consistently positioned COST-G as the leading performer, there are little differences among JPL, CSR, and ITSG, then followed by GFZ, and CNES.

In conclusion, despite variations in error levels among different GRACE/GRACE-FO Level-2 products, these solutions retain value for hydrologic applications, whether on a global scale or at the basin level. Considering the assessments conducted, we recommend the preferential use of COST-G products.

Disclosure statement

No potential conflict of interest was reported by the author(s).

Funding

The work was supported by the Danmarks Frie Forskningsfond [10.46540/2035-00247B]; National Natural Science Foundation of China [12261131504]; Natural Science Foundation of Hubei Province [2024AFB108]; Hubei Natural Science Joint Foundation [2023AFD060]; the open fund of State Key Laboratory of Geodesy and Earth's Dynamics [SKLGED2024-1-2, SKLGED2022-2-4]; Science and Technology Research Project of Hubei Provincial Department of Education [Q20232607]; United States Agency for International Development [CA 72038621CA0000].

Data availability statement

GRACE/GRACE-FO datasets are available from the International Centre for Global Earth Models (ICGEM), (http://icgem.gfz-potsdam.de/home).

References

Awange, J. L., Ferreira, V. G., Forootan, E., Andam-Akorful, S. A., Agutu, N. O., & He, X. F. (2016). Uncertainties in remotely sensed precipitation data over Africa. *International Journal of Climatology*, *36*(1), 303–323. https://doi.org/10.1002/joc.4346

Chambers, D. P. & Bonin, J. A. (2012). Evaluation of release-05 GRACE time-variable gravity coefficients over the ocean. *Ocean Science*, *8*(5), 859–868. https://doi.org/10.5194/os-8-859-2012

Chen, J., Cazenave, A., Dahle, C., Llovel, W., Panet, I., Pfeffer, J., & Moreira, L. (2022). Applications and challenges of GRACE and GRACE follow-on satellite gravimetry. *Surveys in*

Geophysics, *43*(1), 305–345. https://doi.org/10.1007/s10712-021-09685-x

Chen, Q., Shen, Y., Kusche, J., Chen, W., Chen, T., & Zhang, X. (2021). High-resolution GRACE monthly spherical harmonic solutions. *Journal of Geophysical Research: Solid Earth*, *126*(1), e2019JB018892. https://doi.org/10.1029/2019JB018892

Cheng, M., Ries, J. C., & Tapley, B. D. (2011). Variations of the Earth's figure axis from satellite laser ranging and GRACE. *Journal of Geophysical Research: Solid Earth*, *116*(B1), 116 (B1). https://doi.org/10.1029/2010JB000850

Daniel, E. B., Camp, J. V., LeBoeuf, E. J., Penrod, J. R., Dobbins, J. P., & Abkowitz, M. D. (2011). Watershed modeling and its applications: A state-of-the-art review. *Open Hydrology Journal*, *5*(1), 26–50. https://doi.org/10.2174/1874378101105010026

Eicker, A., Forootan, E., Springer, A., Longuevergne, L., & Kusche, J. (2016). Does GRACE see the terrestrial water cycle "intensifying"? *Journal of Geophysical Research: Atmospheres*, *121*(2), 733–745. https://doi.org/10.1002/2015JD023808

Ferreira, V. G., Montecino, H. D. C., Yakubu, C. I., & Heck, B. (2016). Uncertainties of the gravity recovery and climate experiment time-variable gravity-field solutions based on three-cornered hat method. *Journal of Applied Remote Sensing*, *10*(1), 015015. https://doi.org/10.1117/1.JRS.10.015015

Forootan, E., Khaki, M., Schumacher, M., Wulfmeyer, V., Mehrnegar, N., van Dijk, A. I., Brocca, L., Farzaneh, S., Akinluyi, F., Ramillien, G., & Shum, C. K. (2019). Understanding the global hydrological droughts of 2003–2016 and their relationships with teleconnections. *Science of the Total Environment*, *650*, 2587–2604. https://doi.org/10.1016/j.scitotenv.2018.09.231

Galindo, F. J., & Palacio, J. (1999, December 9) Estimating the instabilities of N correlated clocks. In Proceedings of the 31th annual Precise Time and Time Interval Systems and Applications Meeting (pp. 285–296).

Huang, Y., Salama, M. S., Krol, M. S., Su, Z., Hoekstra, A. Y., Zeng, Y., & Zhou, Y. (2015). Estimation of human-induced changes in terrestrial water storage through integration of GRACE satellite detection and hydrological modeling: A case study of the Yangtze river basin. *Water Resources Research*, *51*(10), 8494–8516. https://doi.org/10.1002/2015WR016923

Jäggi, A., Meyer, U., Lasser, M., Jenny, B., Lopez, T., Flechtner, F., Dahle, C., Förste, C., Mayer-Gürr, T., Kvas, A., & Lemoine, J. M. (2020). International combination service for time-variable gravity fields (COST-G) start of operational phase and future perspectives. In *Beyond 100: The Next Century in Geodesy: Proceedings of the IAG General Assembly*, Montreal, Canada, July 8–18, 2019 (pp. 57–65). Springer International Publishing.

Khandu, Forootan, E., Schumacher, M., Schumacher, M., Awange, J. L., & Müller Schmied, H. (2016). Exploring the influence of precipitation extremes and human water use on total water storage (TWS) changes in the Ganges-Brahmaputra- Meghna river Basin. *Water Resources Research*, *52*(3), 2240–2258. https://doi.org/10.1002/2015WR018113

Koot, L., De Viron, O., & dehant, V. (2006). Atmospheric angular momentum time-series: Characterization of their internal noise and creation of a combined series. *Journal of Geodesy*, *79*(12), 663–674. https://doi.org/10.1007/s00190-005-0019-3

Kusche, J., Eicker, A., Forootan, E., Springer, A., & Longuevergne, L. (2016). Mapping probabilities of extreme continental water storage changes from space gravimetry. *Geophysical Research Letters*, *43*(15), 8026–8034. https://doi.org/10.1002/2016GL069538

Kusche, J., Schmidt, R., Petrovic, S., & Rietbroek, R. (2009). Decorrelated GRACE time-variable gravity solutions by GFZ, and their validation using a hydrological model. *Journal of Geodesy*, *83*(10), 903–913. https://doi.org/10.1007/s00190-009-0308-3

Kvas, A., Behzadpour, S., Ellmer, M., Klinger, B., Strasser, S., Zehentner, N. & Mayer-Gürr, T. (2019). Itsg-Grace2018: Overview and evaluation of a new grace-only gravity field time series. *Journal of Geophysical Research: Solid Earth*, *124*(8), 9332–9344. https://doi.org/10.1029/2019JB017415

Landerer, F. W., Flechtner, F. M., Save, H., Webb, F. H., Bandikova, T., Bertiger, W. I., Bettadpur, S. V., Byun, S. H., Dahle, C., Dobslaw, H., & Fahnestock, E. (2020). Extending the global mass change data record: GRACE Follow-on instrument and science data performance. *Geophysical Research Letters*, *47*(12). https://doi.org/10.1029/2020GL088306

Lemoine, J. M., Biancale, R., Reinquin, F., Bourgogne, S., & Gégout, P. (2019). CNES/GRGS RL04 Earth gravity field models, from GRACE and SLR data.

Long, D., Pan, Y., Zhou, J., Chen, Y., Hou, X., Hong, Y., Scanlon, B. R., & Longuevergne, L. (2017). Global analysis of spatiotemporal variability in merged total water storage changes using multiple GRACE products and global hydrological models. *Remote Sensing of Environment*, *192*, 198–216. https://doi.org/10.1016/j.rse.2017.02.011

Loomis, B. D., Rachlin, K. E., Wiese, D. N., Landerer, F. W., & Luthcke, S. B. (2020). Replacing GRACE/GRACE-FO C30 with satellite laser ranging: Impacts on Antarctic ice sheet mass change. *Geophysical Research Letters*, *47*(3), e2019GL085488. https://doi.org/10.1029/2019GL085488

Meyer, U., Jäggi, A., Jean, Y., & Beutler, G. (2016). AIUB-RL02: An improved time-series of monthly gravity fields from GRACE data. *Geophysical Journal International*, *205*(2), 1196–1207. https://doi.org/10.1093/gji/ggw081

Peltier, W. R., Argus, D. F., & Drummond, R. (2015). Space geodesy constrains ice age terminal deglaciation: The global ICE-6G_C (VM5a) model. *Journal of Geophysical Research: Solid Earth*, *120*(1), 450–487. https://doi.org/10.1002/2014JB011176

Pokhrel, Y., Felfelani, F., Satoh, Y., Boulange, J., Burek, P., Gädeke, A., Gerten, D., Gosling, S. N., Grillakis, M., Gudmundsson, L., Hanasaki, N., Kim, H., Koutroulis, A., Liu, J., Papadimitriou, L., Schewe, J., Müller Schmied, H., Stacke, T. … Zhao, F. (2021). Global terrestrial water storage and drought severity under climate change. *Nature Climate Change*, *11*(3), 226–233. https://doi.org/10.1038/s41558-020-00972-w

Ran, J. J., Xu, H. Z., & Zhong, M. (2014). Global temporal gravity filed recovery using GRACE data. *Chinese Journal of Geophysics*. https://doi.org/10.6038/cjg20140402

Rodell, M., Velicogna, I., & Famiglietti, J. S. (2009). Satellite-based estimates of groundwater depletion in India. *Nature*, *460*(7258), 999–1002. https://doi.org/10.1038/nature08238

Sasgen, I., Martinec, Z., & Fleming, K. (2007). Wiener optimal combination and evaluation of the gravity recovery and climate experiment (GRACE) gravity fields over Antarctica. *Journal of Geophysical Research: Solid Earth*, *112*(B4), 112 (B4). https://doi.org/10.1029/2006JB004605

Scanlon, B. R., Zhang, Z., Save, H., Wiese, D. N., Landerer, F. W., Long, D., Longuevergne, L., & Chen, J. (2016). Global evaluation of new GRACE mascon products for hydrologic

applications. *Water Resources Research*, *52*(12), 9412–9429. https://doi.org/10.1002/2016WR019494

Steffen, H., Petrovic, S., Müller, J., Schmidt, R., Wünsch, J., Barthelmes, F., & Kusche, J. (2009). Significance of secular trends of mass variations determined from GRACE solutions. *Journal of Geodynamics*, *48*(3–5), 157–165. https://doi.org/10.1016/j.jog.2009.09.029

Stoffelen, A. (1998). Toward the true near-surface wind speed: Error modeling and calibration using triple collocation. *Journal of Geophysical Research Atmospheres*, *103*(C4), 7755–7766. https://doi.org/10.1029/97JC03180

Sun, Y., Riva, R., & Ditmar, P. (2016). Optimizing estimates of annual variations and trends in geocenter motion and J2 from a combination of GRACE data and geophysical models. *Journal of Geophysical Research: Solid Earth*, *121*(11), 8352–8370. https://doi.org/10.1002/2016JB013313

Tapley, B. D., Bettadpur, S., Ries, J. C., Thompson, P. F., & Watkins, M. M. (2004). GRACE measurements of mass variability in the Earth system. *Science*, *305*(5683), 503–505. https://doi.org/10.1126/science.1099192

Tavella, P., & Premoli, A. (1994). Estimating the instabilities of N clocks by measuring differences of their readings. *Metrologia*, *30*(5), 479. https://doi.org/10.1088/0026-1394/30/5/003

Trabucco, A., & Zomer, R. (2019). Global aridity index and potential evapotranspiration (ET0). *Climate Database*, *2*. https://doi.org/10.6084/m9.figshare.7504448.v3

Valty, P., De Viron, O., Panet, I., Van Camp, M., & Legrand, J. (2013). Assessing the precision in loading estimates by geodetic techniques in Southern Europe. *Geophysical Journal International*, *194*(3), 1441–1454. https://doi.org/10.1093/gji/ggt173

Wahr, J., Molenaar, M., & Bryan, F. (1998). Time variability of the Earth's gravity field: Hydrological and oceanic effects and their possible detection using GRACE. *Journal of Geophysical Research: Solid Earth*, *103*(B12), 30205–30229. https://doi.org/10.1029/98JB02844

Wang, C. Q., Xu, H. Z., & Zhong, M. (2015). An investigation on GRACE temporal gravity field recovery using the dynamic approach. *Chinese Journal of Geophysics*. https://doi.org/10.6038/cjg20150306

Wu, X., Feng, X., Wang, Z., Chen, Y., & Deng, Z. (2023). Multi-source precipitation products assessment on drought monitoring across global major river basins. *Atmospheric Research*, *295*, 106982. https://doi.org/10.1016/j.atmosres.2023.106982

Wu, X., Guo, S., Qian, S., Wang, Z., Lai, C., Li, J., & Liu, P. (2022). Long-range precipitation forecast based on multipole and preceding fluctuations of sea surface temperature. *International Journal Climatology*, *42*(15), 8024–8039. https://doi.org/10.1002/joc.7690

Yao, C., Li, Q., Luo, Z., Wang, C., Zhang, R., & Zhou, B. (2019). Uncertainties in grace-derived terrestrial water storage changes over mainland China based on a generalized three-cornered hat method. *Chinese Journal of Geophysics*, *62*(3), 883–897. https://doi.org/10.6038/cjg2019L0454

Zhang, L., Yi, S., Wang, Q., Chang, L., Tang, H. & Sun, W. (2019). Evaluation of GRACE mascon solutions for small spatial scales and localized mass sources. *Geophysical Journal International*, *218*(2), 1307–1321. https://doi.org/10.1093/gji/ggz198

Zhou, H., Luo, Z., Zhou, Z., Zhong, B., & Hsu, H. (2017). HUST-Grace2016s: A new GRACE static gravity field model derived from a modified dynamic approach over a 13-year observation period. *Advances in Space Research*, *60*(3), 597–611. https://doi.org/10.1016/j.asr.2017.04.026